

SOLDER BALL JOINT RELIABILITY WITH ELECTROLESS NI/PD/AU PLATING -INFLUENCE OF ELECTROLESS PD PLATING FILM THICKNESS

Yoshinori Ejiri, Takehisa Sakurai,
Yoshinori Arayama, Yoshiaki Tsubomatsu, Kiyoshi Hasegawa
Hitachi Chemical Co., Ltd.
Ibaraki, Japan
y-ejiri@hitachi-chem.co.jp

ABSTRACT

The influence of Pd film thickness in electroless Ni/Pd/Au plating on the solder ball joint reliability after reflow cycles and thermal aging was investigated by conducting a high-speed solder ball shear test. Sn-3.0Ag-0.5Cu (SAC305) was used as the solder ball in this study. On the basis of the solder joint reliability obtained after multiple reflow cycles and thermal aging, the optimum thickness of the Pd film was found to be 0.05–0.2 μm .

The covering property of electroless Pd plating film on the electroless Ni plating film was also investigated. We found that an electroless Pd plating film with a thickness of 0.02 μm or more covered the electroless Ni plating film adequately, and the solder ball joint reliability in this case was better than that with electroless Ni/Au plating. We consider that the shape of the intermetallic compounds (IMCs) is one of the factors that influence the solder joint reliability after multiple reflow cycles. Consequently, we inferred that the high adhesion at the dendrite layers of IMCs/solder interface resulted in excellent solder ball joint reliability after the reflow cycles. We consider that the thickness of the IMCs is one of the factors that influence the solder joint reliability after thermal aging. In (Cu, Ni, Pd)₆Sn₅ IMCs that contained trace amounts of Pd, the growth of the IMCs is prevented by Pd, resulting in excellent solder ball joint reliability after thermal aging.

Key words: Electroless Ni/Pd/Au, Solder joint reliability, Intermetallic compounds (IMCs), Reflow cycles, Thermal aging, High-speed solder ball shear test

INTRODUCTION

With the widespread use of portable electronic equipment, chip scale packages (CSPs) and ball grid arrays (BGAs) mounted on high-density printed circuit boards (PCBs) have become popular as semiconductor package assemblies. The CSPs and BGAs are connected to the PCBs using solder balls. Such connection methods require smaller connection areas and no metal leads, thus resulting in a lower ability to resist the stress relaxation than in the case of the traditional methods of connecting the leads of thin small outline packages (TSOP) and quad flat packages (QFPs). The connection methods employing solder balls, therefore, involve many problems related to

joint reliability. Several studies on the reliability of solder ball joint connections with CSPs and BGAs are now in progress¹⁻¹⁶.

The conventional electrolytic Ni/Au plating is a mature technology that has long been used for surface finishing of package substrates. However, this technique cannot be applied to high-density package substrates, because it requires bus lines to each terminal and the necessary area for those lines. Therefore, electroless Ni/Au plating was adopted because it does not require bus lines. However, drop tests revealed that the reliability of ball joints prepared by this technique is insufficient. To solve this problem, electroless Ni/Pd/Au plating was adopted for surface finishing of the terminals of package substrates¹⁷⁻¹⁹.

Recently, electroless Ni/Pd/Au plating is being offered as an alternative surface finishing process with high solder joint reliability and wire bondability. In the previous studies, the details regarding the influence of Pd thickness on solder joint reliability and IMC growth have not been provided. In this study, the influence of Pd film thickness on solder ball joint reliability was investigated to clearly identify the optimum thickness of the Pd film in electroless Ni/Pd/Au plating.

EXPERIMENTS

Sample Preparation

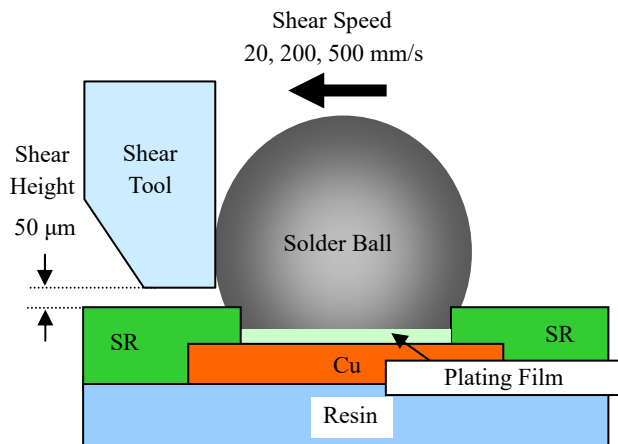
A test pattern was formed on an epoxy resin copper cladding laminate (MCL-E-679F; Hitachi Chemical Co., Ltd.) using the semi-additive method. The thicknesses of the board and copper pad were 0.6 mm and 25 μm , respectively. Then, solder resist was formed with a solder mask using a photo-definable type resist. The opening diameter of the ball pad was 0.45 mm. These test substrates were covered with electroless Ni/Au (ENIG: electroless Ni/immersion Au) and electroless Ni/Pd/Au (ENEPIG: electroless Ni/electroless Pd/immersion Au) plating. After applying flux, solder balls (SAC305) were attached to the test substrates and passed through a nitrogen-reflow furnace. The thickness of each plating film and the evaluation conditions are listed in Table 1.

Reliability Test on Solder Ball Joints (High-Speed Shear)

As shown in Fig. 1, the distance between the shear tool tip

Table 1. Experimental Conditions

Surface Finishes	Electroless Ni(5 μm)/Au(0.03 μm)	
	Electroless Ni(5 μm)/Pd*/Au(0.03 μm)	
Pd* Thickness	0.005, 0.01, 0.015, 0.02, 0.03, 0.05, 0.1, 0.2, 0.3, 0.5 μm	
Solder Ball	Sn-3.0Ag-0.5Cu(φ0.76 mm)	
Evaluation Conditions	Reflow Cycles	1, 3, 7(Max Temp.: Sn-3.0Ag-0.5Cu 252 °C)
	Thermal Aging at 150 °C	100, 300, 500, 1000 h
Equipment	DAGE 4000HS Bond Tester (Dage Precision Industries, LTD.)	
Shear Speed	20, 200, 500 mm/s	
Classification of the Fracture Mode (Solder Residual Rate)	Mode A: 100%, Mode B: 50~99%, Mode C: 10~49%, Mode D: 0~9%	

**Figure 1.** Outline of Solder-Ball Shear Test

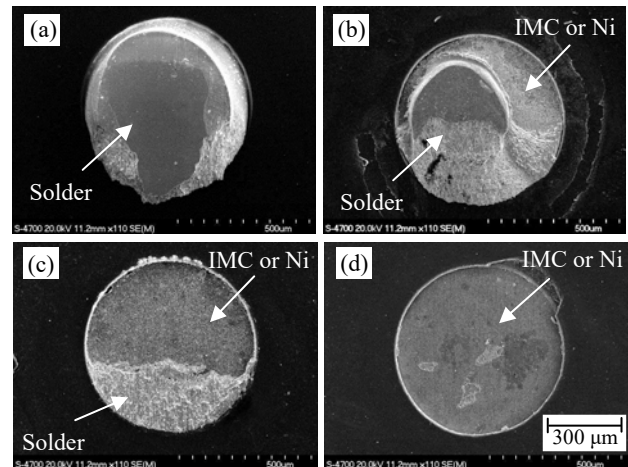
and the package substrate was 50 μm. The shear speeds were 20, 200, and 500 mm/s. A high-speed bond tester 4000HS (Dage Precision Industries, Ltd.) was used (Fig. 2). The fracture surface was observed with an optical microscope, and the fracture modes were classified into four failure modes. Typical images of these four failure modes are shown in Fig. 3.

Method of Evaluating the Covering Property of Pd Plating Film on Ni Plating Film

To evaluate the covering property of the Pd plating film on the Ni plating film, ultrasonic waves (1 min, 20 kHz) were applied to the Pd plated specimens to detect the low adhesion points. The surface of the Pd plated specimens before and after applying ultrasonic waves was observed using a scanning electron microscope (SEM). The cross section of these specimens was observed using a transmission electron microscope (TEM).

Growth of IMCs depending on Pd Film Thickness

The growth of the IMCs, corresponding to different Pd film thicknesses, was observed using an SEM, and the composition of the IMCs was analyzed by energy dispersive X-ray spectroscopy (EDX).

**Figure 2.** Externals of High-speed Shear Test Equipment (DAGE 4000HS Bond Tester)**Figure 3.** Classification of the Fracture Mode for Solder Ball Shear Test

- (a) Mode A: Solder residual rate 100%,
- (b) Mode B: Solder residual rate 50~99%,
- (c) Mode C: Solder residual rate 10~49%,
- (d) Mode D: Solder residual rate 0~9%

RESULTS AND DISCUSSION

Results of High-Speed Solder Ball Shear Test

The influence of electroless Pd film thickness on solder ball joint reliability was investigated. The results of the high-speed solder ball shear test are shown in Figs. 4 and 5.

Almost all the samples with electroless Ni/Au film (Fig. 4a) showed brittle fracture in each evaluated condition. The solder joint reliability with the electroless Pd film having a thickness of 0.01–0.03 μm was higher than that with the electroless Ni/Au films. In the case of electroless Pd films with thickness more than 0.3 μm , the percentage of ductile fracture mode failures (Mode A) decreased with increasing

number of reflow cycles and higher Pd film thickness. The reliability of the solder ball joint with a 0.05–0.2 μm thick electroless Pd film was similar to that obtained with conventional electrolytic Ni/Au¹⁹⁾ films. Thus, the optimum thickness of an electroless Pd film for a reliable solder ball joint was found to be 0.05–0.2 μm .

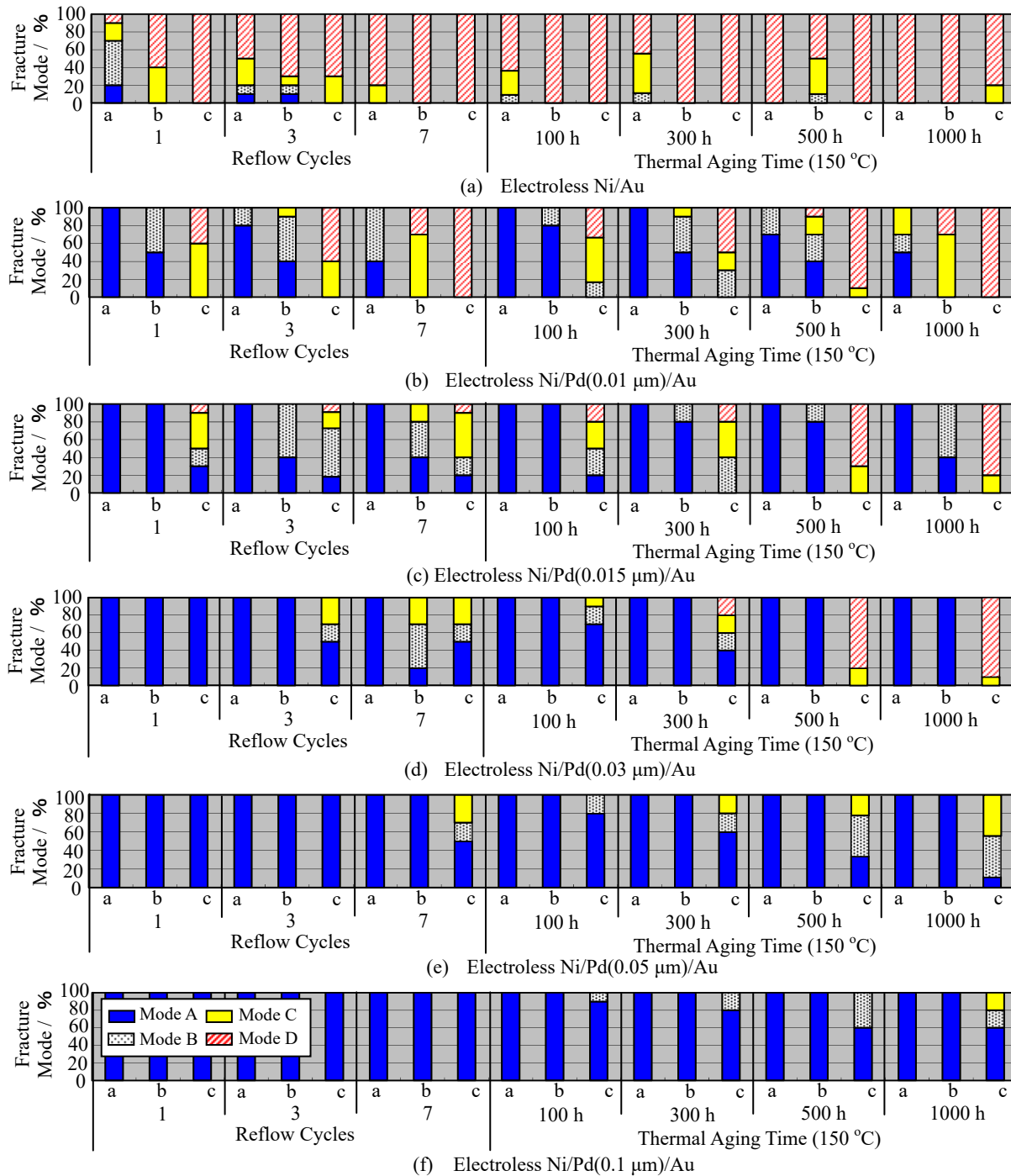


Figure 4. Dependence of Fracture Modes on Pd Thickness

Shear speed: a 20 mm/s, b 200 mm/s, c 500 mm/s

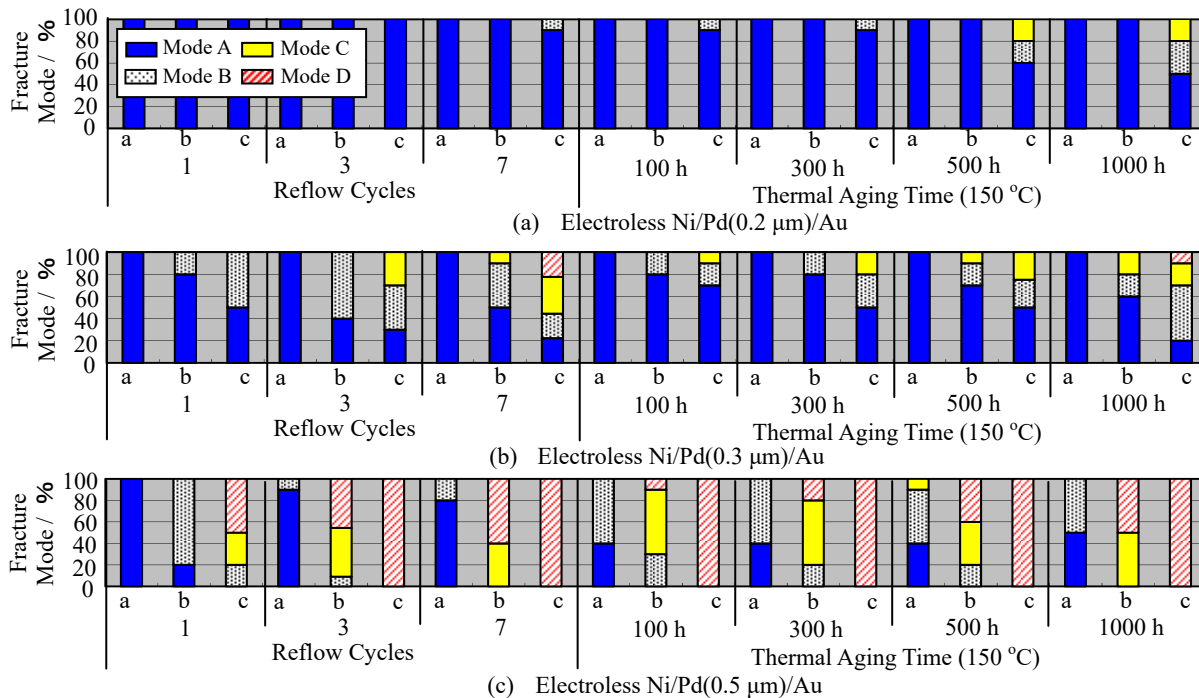


Figure 5. Dependence of Fracture Modes on Pd Thickness
Shear speed: a 20 mm/s, b 200 mm/s, c 500 mm/s

Covering Property of Pd Plating Film on Ni Plating Film

Fig. 6 shows the results of SEM observations with different Pd thicknesses before and after applying ultrasonic waves. In the case of 0.01–0.015 μm thick electroless Pd film, pinholes occurred after applying ultrasonic waves. In contrast, in the case of electroless Pd films with thickness more than 0.02 μm, there were no pinholes after applying ultrasonic waves. A model depicting the covering process of Pd plating film on the Ni plating film is shown in Fig. 7. The initial stage of Pd deposition on the electroless Ni surface involves a replacement reaction (Fig. 7a). Since the electroless Pd plating bath includes a reducing agent, corrosion hardly occurs, because the reduction reaction progresses immediately on the Pd film plated by the replacement reaction (Fig. 7b). However, the covering of the Pd film at the replacement reaction points was delayed compared to the other points. Thin Pd plated points existed in the case of 0.01–0.015 μm thick Pd film (Figs. 7c and 7d). It is presumed that the thin Pd plated points might be the cause of occurrence of the pinholes.

All the samples with electroless Ni/Au film showed brittle fracture in each of the evaluated conditions. The SEM images of surface morphology of the electroless Ni film, after the dissolution of Au or Pd, are shown in Fig. 8. In the case of electroless Ni/Pd/Au film, no corrosive pits were formed in the Ni layers, as shown in Fig. 8(a). On the other hand, in the case of electroless Ni/Au film, low reliability was observed, because of the formation of corrosive pits in the layers of electroless Ni, caused by the dissolution of Ni

during the immersion plating of Au (Fig. 8b)¹⁷. The TEM images of the cross section of the electroless plating film are shown in Fig. 9. In the cross section of the electroless Ni/Pd/Au film with 0.02 μm thickness of Pd (Fig. 9a), there were no local corrosive pits at the interface between the electroless Pd and electroless Ni. We found that 0.02 μm thick electroless Pd film can be considered as an effective barrier film to prevent the Ni layer from dissolving during immersion plating of Au. However, in the case of electroless Ni/Au film (Fig. 9b), the surface of the electroless Ni was found to have dissolved evenly during the immersion gold plating.

The cross-sectional views of the plating film and solder joint interface for various Pd thicknesses are shown in Fig. 10. In the case of electroless Ni/Au film (Fig. 10a), the surface of electroless Ni was corroded by the immersion gold plating. IMC layers were formed at the interface of solder and the corroded electroless Ni during the reflow process. The corroded electroless Ni layer is the cause of the poor adhesion at the Ni/IMCs interface. Therefore, the brittle fracture may easily occur in the case of electroless Ni/Au film. In the case of 0.005–0.015 μm thick Pd film (Fig. 10b), the thin Pd plating points were attacked by the immersion gold plating, and there was local corrosion in the electroless Ni layer. The joints with 0.005–0.015 μm thick Pd film were better than those with electroless Ni/Au film. With a Pd film thickness of 0.02 μm or more (Fig. 10c), the absence of corrosive pits in the Ni layers might have contributed to excellent solder joint reliability.

Pd Thickness (μm)	As Plating	After Ultrasonic Cleaning	Pd Thickness (μm)	As Plating	After Ultrasonic Cleaning
0		Ni 	0.015		Pinhole
0.005			0.02		Pd
0.01		Pinhole 	0.03		

Figure 6. Coverage of the Electroless Pd Plating Film on Electroless Ni Plating Film

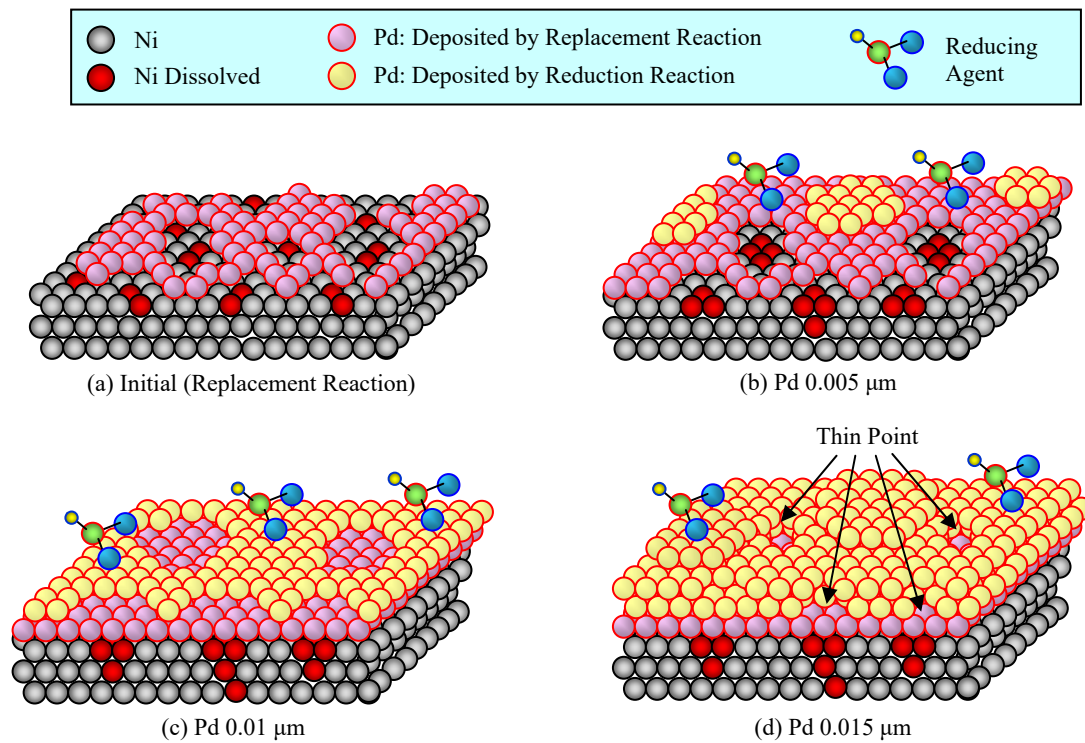


Figure 7. A Model Depicting the Covering Process of Pd Plating Film on the Ni Plating Film

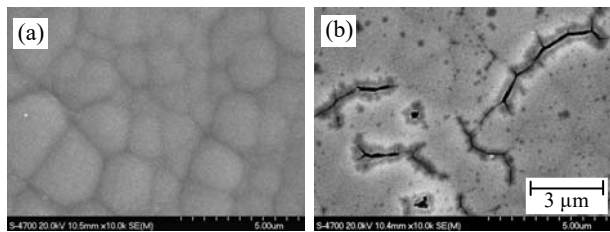


Figure 8. SEM Photographs of Surface Morphology of the Electroless Ni after the Dissolution of Au or Pd
(a) Electroless Ni/Pd/Au, (b) Electroless Ni/Au

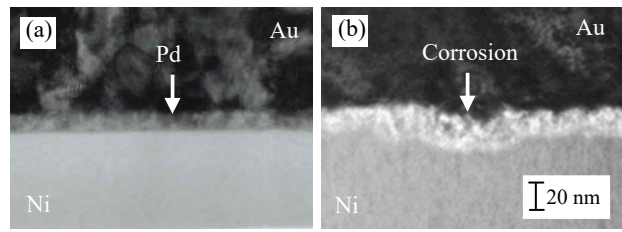


Figure 9. TEM Photographs of Cross-section of the Electroless Plating Film
(a) Electroless Ni/Pd/Au, (b) Electroless Ni/Au

Items	Pd Thickness		
	(a) 0 μm	(b) 0.005~0.015 μm	(c) ≤0.02 μm
Cross-sectional Images of Plating Film			
Cross-sectional Images of Solder Joint			
Solder Joint Reliability	Low	Middle	High

Figure 10. Cross-sectional Models of Plating Film and Solder Joint Interface depending on Pd Thickness

Growth of the IMCs at the Solder Ball Joint Interface

(1) Influence of reflow cycles

The SEM observations of the cross sections of the IMCs for various Pd thicknesses and reflow cycles are shown in Fig. 11. When the Pd thickness was 0.015–0.3 μm, dendrite layers of IMCs were formed at the interface of SAC305 and the Ni plating film. On the other hand, when the Pd thickness was 0.5 μm, flat layers of IMCs were formed.

To investigate the growth of the IMCs in greater detail, the cross section and surface morphology of the IMCs after the reflow cycles were observed on 0.1 μm and 0.5 μm thick Pd films. The results are shown in Fig. 12. When the thickness was 0.1 μm, thin dendrite layers of (Cu, Ni, Pd)₆Sn₅ IMCs were formed after one reflow cycle. The size of the dendrite layers of the IMCs increased with increasing number of reflow cycles. After seven reflow cycles, thick dendrite layers of (Cu, Ni, Pd)₆Sn₅ IMCs [Fig. 12 I (Cu : Ni : Pd : Sn=23.5 : 18.1 : 0.2 : 58.2 wt%)] were formed.

In the case of 0.5 μm thick Pd film, two types of IMC compositions were observed: one is (Cu, Ni, Pd)₆Sn₅

[Fig. 12 II (Cu : Ni : Pd : Sn=23.4 : 16.5 : 1.2 : 59.0 wt%)], and the other is Cu/Ni/Pd/Sn [Fig. 12 III (Cu : Ni : Pd : Sn=1.4 : 3.4 : 11.1 : 84.1 wt%)]. The shape of (Cu, Ni, Pd)₆Sn₅ IMCs was granular. These results suggested that the Cu/Ni/Pd/Sn IMCs, which included a high concentration of Pd, affected the shape of (Cu, Ni, Pd)₆Sn₅ IMCs. After seven reflow cycles, (Cu, Ni, Pd)₆Sn₅ IMCs increased in size and showed a more planar morphology [Fig. 12 IV (Cu : Ni : Pd : Sn=23.3 : 16.5 : 0.8 : 59.4 wt%)].

The cross-sectional views of the IMCs for various Pd thicknesses and reflow cycles are shown in Fig. 13. In the case of 0.1 μm thick Pd film, the size of the dendrite layers of IMCs increased with increasing number reflow cycles. We considered that the high adhesion at the dendrite layers of IMCs/solder interface resulted in an excellent joint after multiple reflow cycles. In the case of 0.5 μm thick Pd film, the IMC phase growth showed a more planar morphology after multiple reflow cycles. The poor adhesion at the plane IMCs/solder interface may be the reasons for the decrease in solder joint reliability.

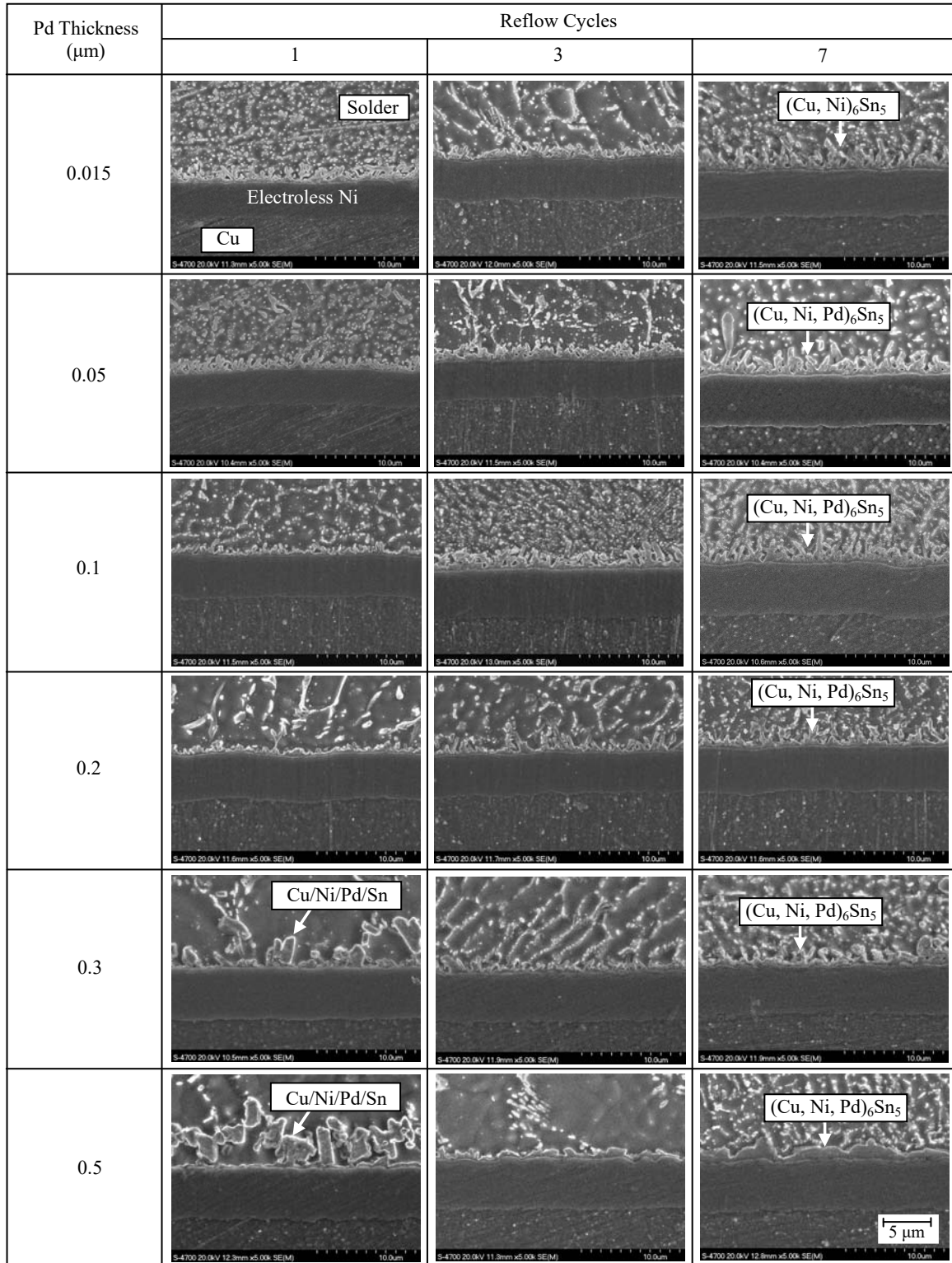


Figure 11. Cross Section of IMCs depending on Pd Thickness and Reflow Cycles

Pd Thickness (μm)	Item	Reflow Cycles		
		1	3	7
0.1	Cross Section			
	Surface (Solder Removed)			
0.5	Cross Section			
	Surface (Solder Removed)			

Figure 12. Cross Section and Surface Morphology of IMCs after Reflow Cycles with 0.1 μm and 0.5 μm thick Pd films

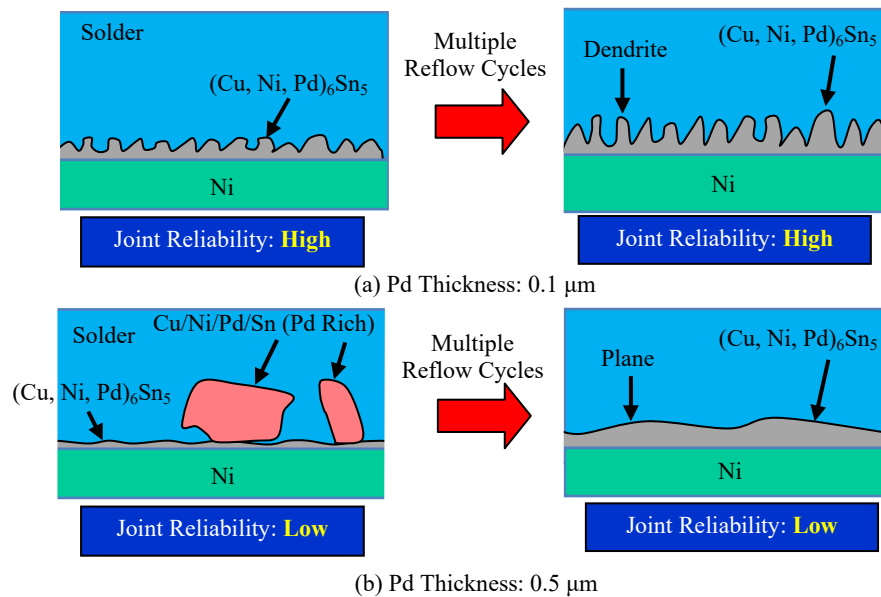


Figure 13. Cross Sectional Models of the IMCs depending on Pd Thickness and Reflow Cycles

(2) Influence of thermal aging

The level of reliability of the solder ball joint with a 0.1 μm thick electroless Pd film (Fig. 4f) was better than that obtained with a 0.03 μm thick electroless Pd film (Fig. 4d) after 1000 h of thermal aging. Therefore, the root cause of excellent solder joint reliability with a 0.1 μm thick electroless Pd film after thermal aging was investigated.

The cross section and surface morphology of the IMCs after thermal aging were observed with 0.03 μm and 0.1 μm thick Pd films. The results are shown in Fig. 14. The IMC phase growth after thermal aging showed a more planar morphology than that after multiple reflow cycles. The IMC layers with 0.1 μm thick Pd film were thinner than those observed in the joints with 0.03 μm thick Pd film. The composition of the IMCs with 0.03 μm and 0.1 μm

thick Pd films were (Cu, Ni)₆Sn₅ [Cu : Ni : Sn=23.5 : 18.1 : 57.4 wt%] and (Cu, Ni, Pd)₆Sn₅ [Cu : Ni : Pd : Sn=24.1 : 17.4 : 0.2 : 58.3 wt%], respectively.

The cross-sectional views of the IMCs for various Pd thicknesses after thermal aging are shown in Fig. 15. In the case of 0.1 μm thick electroless Pd film, (Cu, Ni, Pd)₆Sn₅ IMCs were formed at the solder joint interface, and the growth rate of (Cu, Ni, Pd)₆Sn₅ IMC layers was less than that of (Cu, Ni)₆Sn₅ IMCs with thermal aging. We inferred that the trace amounts of Pd prevented the growth of the IMCs. The IMCs are generally more brittle than the base metal, and it is reported that thick IMCs decrease solder joint reliability²⁰⁻²². We estimate that the thin layer of (Cu, Ni, Pd)₆Sn₅ IMCs with 0.1 μm thick Pd film after thermal aging is the cause of excellent solder ball joint reliability.

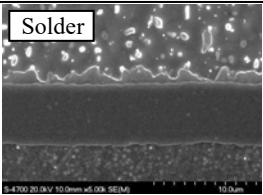
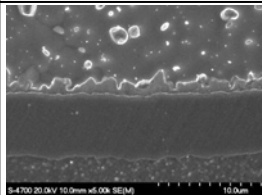
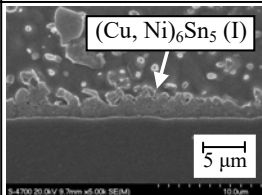
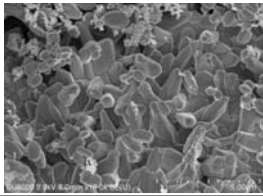
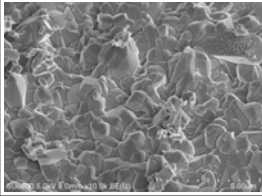
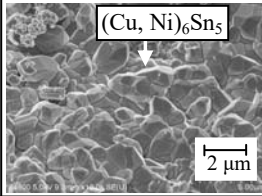
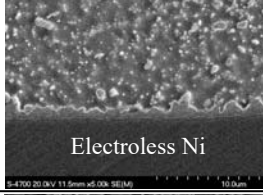
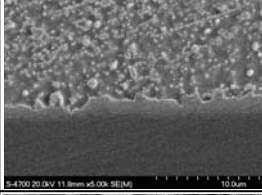
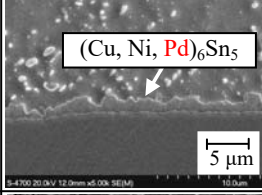
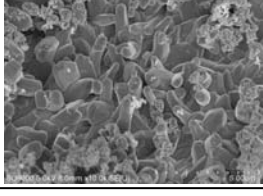
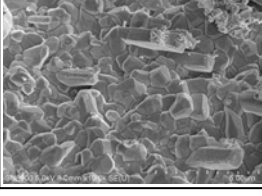
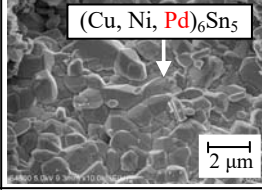
Pd Thickness (μm)	Item	Thermal Aging Time		
		100 h	500 h	1000 h
0.03	Cross Section			
	Surface (Solder Removed)			
0.1	Cross Section			
	Surface (Solder Removed)			

Figure 14. Cross Section and Surface Morphology of IMCs depending on Pd Thickness and Thermal Aging Time

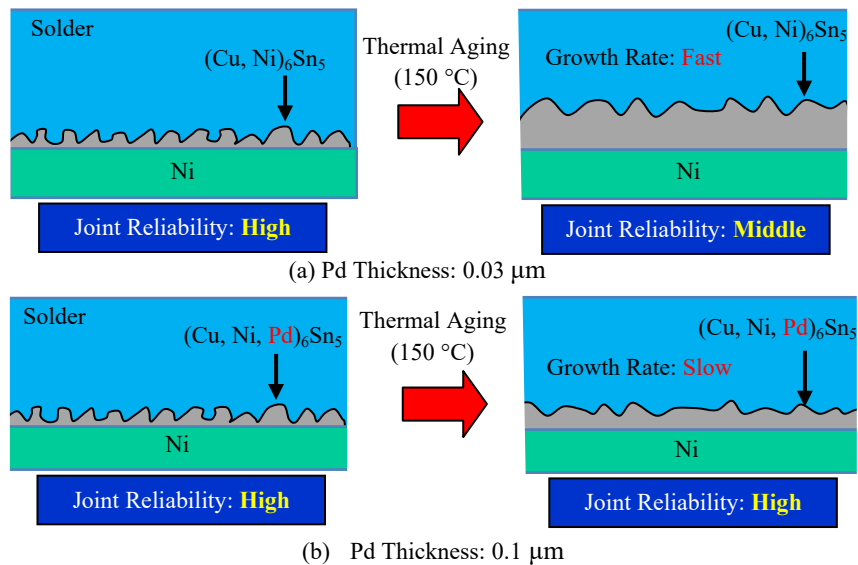


Figure 15. Cross Sectional Models of the IMCs depending on Pd Thickness and Thermal Aging

CONCLUSION

The influence of Pd film thickness in electroless Ni/Pd/Au plating on the solder ball joint reliability was investigated. The following conclusions were obtained.

- (1) Based on the solder joint reliability obtained after multiple reflow cycles and thermal aging, the optimum thickness of Pd film was found to be 0.05–0.2 μm .
- (2) The shape of the IMCs is considered to be one of the factors that influence the solder joint reliability after multiple reflow cycles. We estimated that the high adhesion at the dendrite layers of IMCs/solder interface resulted in excellent joints after multiple reflow cycles.
- (3) The thickness of the IMCs is considered to be one of the factors that influence the solder joint reliability after thermal aging. For $(\text{Cu, Ni, Pd})_6\text{Sn}_5$ IMCs that contained trace amounts of Pd, the growth of the IMCs is prevented by Pd, resulting in excellent solder ball joint reliability after thermal aging.

REFERENCES

- [1] Z. Mei, P. Callery, D. Fisher, F. Hau and J. Glazer, "Interfacial Fracture Mechanism of BGA Package on Electroless Ni/Au," *Advances in Electronic Packaging* 1997, *Proc. Inter Pack '97*, ASME International, New York, NY, 1997, pp. 1543~1550
- [2] Z. Mei, M. Kaufman, A. Eslambolchi and P. Johnson, "Brittle Interfacial Fracture of PBGA Packages Soldered on Electroless Nickel/Immersion Gold," *Proc. 48th Electronic Components & Technology Conference*, New York, NY, 1998, pp. 952~961
- [3] H. Matsuki, H. Ibuka, H. Saka, Y. Araki and T. Kawahara, "TEM Observations of Solder Joints for Electronic Device," *Proc. 3rd IEMT/IMC*, IEEE, New York, NY, 1999, pp. 315~320
- [4] N. Buinno, "A Root Cause Failure Mechanism for Solder Joint Integrity of Electroless Nickel/Immersion Gold Surface Finishes," *Proc. IPC Printed Circuits Expo '99*, IPC, Northbrook, IL, 1999, pp. S18-5-1~5-8
- [5] Z. Mei, P. Johnson, M. Kaufman and A. Eslambolchi, "Effect of Electroless Ni/ Immersion Au Plating Parameters on PBGA Solder Joint Attachment Reliability," *Proc. 49th Electronic Components & Technology Conference*, IEEE, New York, NY, 1999, pp. 125~134
- [6] A. Zribi, R. R. Chromik, R. Presthus, J. Clum, K. Teed, L. Zavalij, J. Devita, J. Tova and E. J. Cotts, "Solder Metallization Interdiffusion In Microelectronic Interconnects," *Proc. 49th Electronic Components & Technology Conference*, IEEE, New York, NY, 1999, pp. 451~457
- [7] P. Backus, K. Johal, D. Metger and H. J. Schreier, "Investigations on Brittle Fracture of BGA Assemblies on Electroless Nickel/ Immersion Gold Surface Finishes," *Proc. IPC Electronic Circuits World 8, Tokyo*, IPC, Northbrook, IL, 1999, pp. PO3-1-1~PO3-1-4
- [8] H. D. Blair, T. Y. Pan and J. M. Nicholson, "Intermetallic Compound Growth on Ni, Au/Ni, and Pd/Ni Substrates with Sn/Pb, Sn/Ag, and Sn Solders," *Proc. 48th Electronic Components & Technology Conference*, IEEE, New York, NY, 1998, pp. 259~267
- [9] R. Ghaffarian, "Effects of Board Surface Finish on Failure Mechanisms and Reliability of BGAs," *Proc. Surface Mount International'98*, 1998, pp. 59~69
- [10] R. W. Johnson, V. Wang and M. Palmer, "Thermal Cycle Reliability of Solder Joints to Alternate Plating Finishes," *Proc. Surface Mount International'98*, 1998, pp. 681~686
- [11] M. N. Islam, Y. C. Chan, A. Shaif and M. O. Alam, *Microelectronics Reliability*, **43**, 2031(2003)

- [12] R. J. Coyle, P. P. Solan, A. J. Serafino and A. Gahr: "The influence of Temperature Aging on Ball Shear Strength and Microstructure of Area Array Solder Balls", *Proc. 50th Electronic Components & Technology Conference*, IEEE, Las Vegas, NV, 2000, pp. 160~169
- [13] T. C. Chiu, K. Zeng, R. Stierman, D. Edwards and K. Ano: "Effect of Thermal Aging on Board Level Drop Reliability for Pb-free BGA Packages", *Proc. 54th Electronic Components & Technology Conference*, IEEE, Las Vegas, NV, 2004, pp. 1256~1262
- [14] Lei Wang, Hao Kou, Yexiang Ning, Bei Wang, Xian Lin and Zuyao Liu: "Effect of PCB Surface Finishes on Lead-Free Solder Joint Reliability", *Journal of SMT*, Vol. **23**, No. 4, 2010, pp. 13~23
- [15] Brian Roggeman, Ursula Marquez de Tino and Denis Barbini: "Reliability Investigation of Sn/Cu/Ni Solder Joints", *Proc. SMTA International 2009*, SMTA, San Diego, California, 2009, pp. 447~452
- [16] William Johannes, Paul Vianco, Jerry Rejent and Bonnie McKenzie: "Long Term Reliability of Eutectic Sn-Pb and Pb-Free Solder Joints made to the ENEPIG Surface Finish", *Proc. SMTA International 2012*, SMTA, Orland, Florida, 2012, pp. 980~988
- [17] K. Hasegawa, A. Takahashi, T. Noudou, S. Nakajima, A. Takahashi, M. Nomoto, and A. Nakaso, "Electroless Ni-P/Pd/Au Plating for Semiconductor Package Substrate," *Proc. SMTA International 2000*, SMTA, Edina, MN, 2000, pp. 225~231
- [18] Y. Ejiri, T. Sakurai, Y. Arayama, Y. Tsubomatsu, K. Akai, M. Nakagawa, and K. Hasegawa "Pb Free Solder Joint Reliability of Various Surface Finishes," *Proc. SMTA International 2014*, SMTA, Rosemont, IL, 2014, pp. 1005~1013
- [19] Y. Ejiri, T. Noudou, T. Sakurai, Y. Arayama, Y. Tsubomatsu, and K. Hasegawa "Influence of Surface Finishes and Solder Alloys on Solder Ball Joint Reliability," *Proc. SMTA International 2015*, SMTA, Rosemont, IL, 2015, pp. 957~971
- [20] L. C. Tsao, Evolution of nano-Ag₃Sn particle formation on Cu-Sn intermetallic compounds of Sn_{3.5}Ag_{0.5}Cu composite solder/Cu during soldering, *J. Alloy Compd*, **509**, 2011, pp. 2326~2333.
- [21] L. C. Tsao, Suppressing effect of 0.5 wt.% nano-TiO₂ addition into Sn-3.5Ag-0.5Cu solder alloy on the intermetallic growth with Cu substrate during isothermal aging, *J. Alloy Compd*, **509**, 2011, pp. 8441~8448.
- [22] X.Y. Liu, M.L. Huang, C. M. L. Wu, Lai Wang, Effect of Y₂O₃ particles on microstructure formation and shear properties of Sn-58Bi solder, *J Mater Sci: Mater Electron, J Mater Sci: Mater Electron*, **21**, 2010, pp. 1046~1054.